GEOLOGY | THE GEOLOGICAL SOCIETY OF AMERICA®

https://doi.org/10.1130/G45394.1

Manuscript received 17 July 2018
Revised manuscript received 11 October 2018
Manuscript accepted 14 October 2018

Published online 9 November 2018

Penetration depth of meteoric water in orogenic geothermal systems

Larryn W. Diamond*, Christoph Wanner, and H. Niklaus Waber
Institute of Geological Sciences, University of Bern, Baltzerstrasse 3, CH-3012 Bern, Switzerland

ABSTRACT

Warm springs emanating from deep-reaching faults in orogenic belts with high topography and orographic precipitation attest to circulation of meteoric water through crystalline bedrock. The depth to which this circulation occurs is unclear, yet it is important for the cooling history of exhuming orogens, for the exploitation potential of orogenic geothermal systems, and for the seismicity of regional faults. The orogenic geothermal system at Grimsel Pass, Swiss Alps, is manifested by warm springs with a clear isotopic fingerprint of high-altitude meteoric recharge. Their water composition and their occurrence within a 3 Ma fossil upflow zone render them particularly favorable for estimating the temperature along the deep flow path via geochemical modeling. Because the background geotherm has remained stable at 25 °C/km and other heat sources are unavailable, the penetration depth can be derived from the deep-water temperature. We thus estimated the base of the Grimsel system to be at 230–250 °C and 9–10 km depth. We propose that deep temperatures in such systems, particularly those with normal background geotherms (<30 °C/km), have been systematically underestimated. Consequently, far more enthalpy may be accessible for geothermal energy exploitation around the upflow zones than previously thought. Further, the prevalence of recent earthquake foci at ≤10 km beneath Grimsel suggests that meteoric water is involved in the seismicity of the host faults. Our results therefore call for reappraisal of the heat budget and the role of meteoric water in seismogenesis in uplifting orogens.

INTRODUCTION

Meteoric water circulation in orogenic belts is expressed by thermal springs discharging at temperatures up to 80 °C from deep-reaching faults, e.g., in the Canadian Rocky Mountains (Grasby and Hutcheon, 2001), the Southern Alps of New Zealand (Menzies et al., 2014), and the European Alps (Sonney and Vuataz, 2009). The hydraulic gradients that drive circulation arise from the conjunction of high orographic precipitation, mountainous topography, and permeable faults that link topographic highs with valley floors via the hot bedrock. Knowledge of the maximum possible depth to which meteoric water can infiltrate bedrocks is fundamental to our understanding of how uplifting orogens cool, of how groundwater chemistry evolves in orogenic belts, and of how water catalyzes deformation and seismicity in active orogens. In addition, since the bedrock geotherm supplies the heat to the circulating water, the maximum depth of water penetration defines the maximum temperature attainable by surface springs and their upflow zones, thereby setting limits on their potential for geothermal energy exploitation.

The $\delta^{18}O$ and $\delta^{2}H$ signatures of minerals and fluid inclusions in metamorphic and hydrothermal rocks in orogenic belts occasionally indicate equilibration with isotopically depleted water that can only have had a meteoric origin. Petrologic calculations and structural arguments are typically used to constrain the penetration depths, leading to estimates of 5–23 km (for references, see Table DR1 in GSA Data Repository[1]). If these depths are accurate, then meteoric water would attain temperatures up to ~400 °C. The studies that report the greatest depths explicitly invoke penetration into the ductile deformation regime, for which active processes such as fault-valve behavior would be necessary, since hydraulic gradients cannot drive flow through disconnected paths. In contrast, other workers (e.g., Raimondo et al., 2013) have argued that the isotopic signatures are inherited from pre-orogenic, near-surface alteration of the rocks and that metamorphic dehydration upon deep burial has liberated the isotopically depleted water. Hence, it is currently unclear how deep meteoric water actually penetrates in such systems.

As an alternative approach to this question, we performed geochemical modeling on chemically and isotopically well-characterized thermal waters currently discharging from the Grimsel Pass orogenic geothermal system in the Swiss Alps. This approach bypasses many of the assumptions inherent in the petrologic studies and provides robust evidence that meteoric water has penetrated at least 9–10 km deep into the continental crust to attain temperatures of 230–250 °C.

SITE DESCRIPTION

The Grimsel Pass geothermal system (Fig. 1) is manifested by several low-flow (<10 L/min) warm springs with temperatures up to 28 °C (Pfeifer et al., 1992; Waber et al., 2017) and by two fossil mineralized breccias, each of which is ~0.25 km^2. The springs discharge through one of the breccias into a north-south pipeline tunnel that lies 250 m beneath Grimsel Pass (Figs. 1B and 1C). At 1910 m above sea level (a.s.l.), they are the highest known warm springs in the entire Alps.

The mineralized breccias are subvertical, pipe-like bodies that overprint and link a set of older, subvertical east-northeast–trending ductile shear zones (Fig. 1C). These shear zones are major strike-slip structures in the central Alps, with lengths of several tens of kilometers and seismically indicated vertical extents of >20 km (Belgrano et al., 2016; Herwegh et al., 2017). The brecciated faults are hosted by monotonous granitoids and minor quartzofeldspathic

*E-mail: diamond@geo.unibe.ch

[1]GSA Data Repository item 2018412, chemical analyses of springs and details of analytical and computational methods, is available online at http://www.geosociety.org/datarepository/2018/, or on request from editing@geosociety.org

CITATION: Diamond, L.W., Wanner, C., and Waber, H.N., 2018, Penetration depth of meteoric water in orogenic geothermal systems: Geology, v. 46, p. 1063–1066, https://doi.org/10.1130/G45394.1

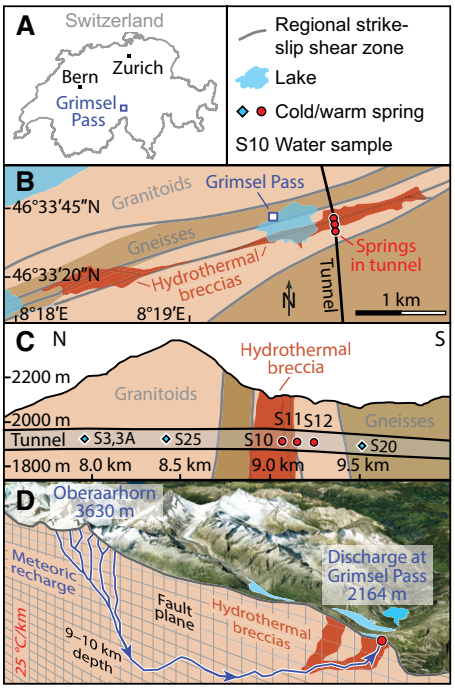

Figure 1. A: Location of Grimsel Pass, Swiss Alps. B: Geological map with tunnel trace showing spatial coincidence among regional strike-slip faults, 3.3 Ma hydrothermal breccias, and currently active warm springs (after Belgrano et al., 2016). C: Geological cross section along tunnel showing sampled springs (labeled Sxx; after Pfeifer et al., 1992). *X* axis is distance from north portal. D: Regional view to north-northwest showing topography and conceptual present-day flow path of meteoric water along subvertical strike-slip fault. Reconstructed deep-water temperature of 230–250 °C corresponds to 9–10 km penetration depth (see text).

gneisses of the Aar Massif, an ~20-km-thick block of Variscan lower continental crust that was overprinted by greenschist-facies metamorphism and uplifted during the Alpine orogeny (Herwegh et al., 2017). Hence, the upflow path of the thermal waters is dominated to great depths by microcline K-feldspar, completely albitized plagioclase, quartz, biotite, muscovite, and accessory chlorite, epidote, calcite, fluorite, and apatite. Slivers of anhydrite-bearing Triassic dolomite may also be present along the flow path, as indicated by the high sulfate concentration in the thermal waters.

The granitic clasts of the fault breccias are hydrothermally altered and cemented by an epithermal assemblage of quartz, microcline, and sulfides (mainly pyrite), locally overgrown by small amounts of fibrous chalcedony, illite, and celadonite (Hofmann et al., 2004). The hydrothermal microcline has been dated at 3.3 ± 0.06 Ma (Hofmann et al., 2004), demonstrating that the geothermal system has been active at the same site, albeit perhaps intermittently, for millions of years. Fission-track and U-Th/He ages in the distal wall rocks (Egli et al., 2018) combined with the current rock uplift rate of ~0.9 km/m.y. (Hofmann et al., 2004) yield a mean recent denudation rate of ~0.75 km/m.y., implying the breccias formed at ~2.5 km depth at 3.3 Ma. Primary fluid inclusions in hydrothermal quartz homogenize at ≤152 °C and show that the hydrothermal minerals precipitated from single-phase water containing 3000 mg/L total dissolved solids (TDS; Hofmann et al., 2004). Intersection of the inclusion isochores with hydrostatic pressure at ~2.5 km depth yields trapping temperatures of 165 ± 5 °C. Stable isotope analyses of the hydrothermal minerals revealed the breccias were mineralized by chemically modified meteoric water (δ^2H of –111‰ to –137‰ and δ^{18}O of –7.5‰ to –11‰ relative to Vienna standard mean ocean water [VSMOW]; Hofmann et al., 2004).

The close spatial and temporal relationships between the warm springs and the breccias allow us to use the mineralogy of the breccia cements as a window into the current state of the geothermal system at ~2.5 km depth. In the absence of any Pliocene–Pleistocene igneous activity in the central Alps, the only source of heat for the thermal water is its wall rocks, which have maintained a regional geothermal gradient of 25 °C/km over the past several million years (Hofmann et al., 2004). The 165 ± 5 °C formation temperature of the breccia at relatively shallow depth thus represents a thermal anomaly due to prolonged ascent of hot water. It follows that the maximum circulation depth of the modified meteoric water must be much greater than 2.5 km, where the background rock temperature is well above 170 °C.

METHODS

Cold and warm springs in the pipeline tunnel were sampled in March 2014, September 2015, and July 2016 (Fig. 1C) and analyzed for their chemical composition, δ^2H and δ^{18}O values, and ^{3}H (bomb-tritium) activity (see the Data Repository for data and methods). The analyses of the warm springs were then corrected for mixing with modern surface waters (exemplified by the cold springs) based on their ^{3}H, Na, and Cl contents (explained in the Data Repository). The chemical evolution of the upwelling thermal end-member water was simulated numerically using the reactive-transport software TOUGHREACT V3 (Xu et al., 2014; see the Data Repository for details).

RESULTS AND DISCUSSION

Water Analyses and Fluid Flow Path

Example analyses of warm and cold springs are given in Table 1, and futher analyses (locations in Fig. 1C) are given in Data Repository Tables DR2 and DR3, including analyses from Pfeifer et al. (1992). These demonstrate that the properties of the springs have remained remarkably stable over the 25 yr of monitoring.

TABLE 1. COMPOSITION OF REPRESENTATIVE SPRINGS

Spring type	Warm	Cold	Thermal* end member
Sample	S10	S25	
Year sampled	2016	2016	
Discharge (L/min)	3.0	n.m.	n.m.
Temperature (°C)	28	3.0	57
Eh (mV)	–125	330	–125
pH (–)	8.86	7.78	8.59
Na^+ (mg/L)	79.7	0.453	172.7
K^+ (mg/L)	6.6	0.67	13.6
Mg^{2+} (mg/L)	0.16	0.201	<0.02
Ca^{2+} (mg/L)	3.9	4.15	3.6
Li^+ (mg/L)	0.2	<0.001	0.4
TIC (mg/L)	14.1	3.3	26.7
SO_4^{2-} (mg/L)	85.8	1.32	185.0
F^- (mg/L)	8.6	0.21	18.5
Cl^- (mg/L)	13.8	0.09	29.9
Si (mg/L)	35.3	1.6	74.9
TDS (mg/L)	248	12	525
$\delta^{18}O_{SMOW}$ (‰)	–14.7	–14.2	–15.3
δ^2H (‰)	–105.8	–100.7	–111.8
^{3}H (TU)	2.6	7.5	0.0
S.I.$_{calcite}$ (–)	–0.1	–1.87	0.15
Cold-water fraction (vol%)*	54	100	0

Note: Calculations are described in the Data Repository (see text footnote 1). TIC—total inorganic carbon; TDS—total dissolved solids; SMOW—standard mean ocean water; S.I.—saturation index.

*Corrected for cold-water fraction (Table DR4 in the Data Repository [see text footnote 1]).

The warm springs are of reduced ($Eh_{Ag/AgCl}$ > –250 mV) Na–SO_4–HCO_3 type, carrying 170–280 mg/L TDS, including elevated contents of Si, K, Li, and F. In contrast, the cold springs are weakly mineralized (<100 mg/L TDS) with oxidized, Ca–HCO_3 character typical of modern surface waters at Grimsel Pass. The ^{3}H, Na, and Cl contents reveal that most of the warm waters have mixed with 50–70 vol% modern surface water prior to discharging in the 250-m-deep tunnel. The remainder of this paper deals with the thermal end-member waters that have been corrected for this mixing (Table 1; Table DR4), referred to hereafter as "thermal waters."

The δ^2H and δ^{18}O values of the thermal waters fall on the local meteoric water line and are depleted compared to the cold springs (Fig. 2). Evidently, surface water has been recharging the geothermal system from an infiltration site at a higher altitude than Grimsel Pass, and possibly during a cooler climate in the past. The local topography rises continuously to >1000 m above the discharge site ~12–14 km to the west along the strike of the water-conducting faults in the Oberaarhorn area (Fig. 1D). Thus, assuming recharge in this western region, the topographic head differential provides the hydraulic force to drive isotopically depleted meteoric water deep into the fault zone, where it is heated and acquires solutes via reaction with the wall rocks and then ascends through the breccia pipes, cooling along the way and finally discharging as mineralized thermal water at Grimsel Pass. Because the thermal

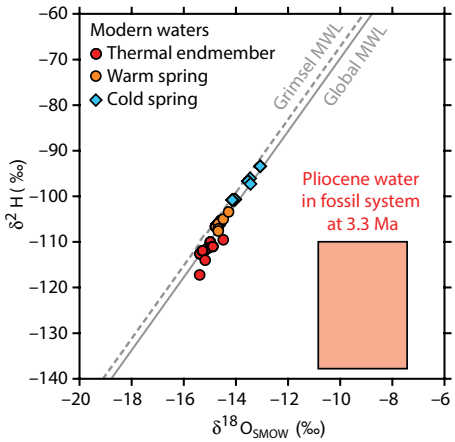

Figure 2. Stable O-H isotope signatures of cold and warm springs and reconstructed end-member thermal waters, all showing close association with meteoric water lines (MWL). Rectangle denotes isotope signatures of fossil system at 3.3 Ma (Hofmann et al., 2004), consistent with meteoric water origin. SMOW—standard mean ocean water.

waters are ^{14}C-free, they must have resided for >30 k.y. within the subsurface flow path (Waber et al., 2017).

Geochemical Modeling

Given the slow flow rates, the long residence time of the circulating water, and the relatively rapid reaction kinetics of silicate minerals at temperature T >> 170 °C (Giggenbach, 1988), it is expected that the thermal water was buffered by equilibrium with its wall rocks along the deep reaches of its flow path. The high-temperature history and chemical maturity of the water are in fact well corroborated by its high Na and K and negligible Mg contents (Table 1; Table DR4). On the other hand, it is expected that the water departed from equilibrium with its wall rocks as it cooled upon ascent, due to increasingly sluggish dissolution-precipitation kinetics, and possibly armoring of the wall rock by quartz and precipitation of low-temperature minerals. In line with this expectation, the only wall-rock minerals that also occur as hydrothermal precipitates in the breccia are microcline and quartz, corresponding to an intermediate level in the upflow path.

Solute geothermometry, as routinely applied to geothermal fluids, aims to find the temperature at which the ascending water departs from equilibrium with its wall rocks, interpreted to represent the minimum reservoir temperature in mature systems (Giggenbach, 1988). Rather than relying on geothermometers calibrated in other geological environments (the results of which are nevertheless given in Table DR4 for comparison), we numerically simulated the specific evolution of the Grimsel thermal water as it rises and cools through its granitic wall rocks. We assumed in the model that the water departs from complete equilibrium with the wall rock at a unique temperature, min-T_{eq}, below which silicate mineral dissolution is suppressed but precipitation is permitted (over a certain temperature interval) according to the computed saturation indices within the multicomponent, multiphase chemical system. Calcite, which reacts much faster than the silicates, is allowed to precipitate and dissolve at all temperatures. Eventually, cooling of the water will kinetically inhibit precipitation of the silicate minerals (e.g., Simmons and Browne, 2000). We suppressed silicate precipitation at the temperature at which the cooling water departs from equilibrium with quartz, denoted T_{qtz}. This temperature was identified by matching the solubility of quartz in the simulations with the mean concentration of $Si_{(aq)}$ in the discharging thermal waters (79.8 mg/L; analogously to classical "quartz thermometry"), yielding a mean T_{qtz} = 165 °C.

Under these constraints, min-T_{eq} was found by iterative forward simulations of the ascending thermal water, such that the final Na/K ratio in the model water at 20 °C matched that observed in the end-member thermal springs at 20 °C. Thus, the mean molal Na/K of 22.7 in the thermal water was obtained when min-T_{eq} was set to 211 °C (Fig. 3A). Quartz and minor microcline precipitate upon cooling between 211 °C and 165 °C (Fig. 3B). The precipitation of microcline lowers the activity of aqueous Al, such that albite remains undersaturated (Fig. 3C) despite its prograde solubility behavior. In contrast, calcite in the wall rocks dissolves along the entire cooling path.

Our simulations are consistent with numerous observations and hence appear to be robust. The computed min-T_{eq} of 211 °C is well above the formation temperature of the breccia, as expected. The simulation also reproduces the occurrence of quartz and microcline in the breccia at ~165 °C, and it predicts pH = 9 at the discharge site, in accord with the actual measurements (Table 1; Table DR2). The reconstructed Na/K ratio of the thermal end-member water is insensitive to the mixing ratio used to correct for cold-water input, because the cold springs contain so little Na and K. In contrast, the Na/K ratio is a very sensitive monitor of min-T_{eq} (Wanner et al., 2014), as demonstrated by the simulation in which min-T_{eq} was set to 230 °C (Fig. 3A), resulting in a predicted Na/K ratio well below that measured in the thermal water. Fluid inclusion analyses show that a high-salinity pore water of 6.5–7 wt% $NaCl_{equiv.}$ was present in the granitic host rock during late Alpine metamorphism (Hofmann et al., 2004). In principle, mixing of this water with a hotter upwelling meteoric water could lower the apparent min-T_{eq}. However, owing to the long lifetime of the Grimsel Pass system (3.3. m.y.) and its high total flux (indicated by the abundance of hydrothermal minerals in the breccias), this metamorphic fluid has evidently been flushed out of the flow path, as

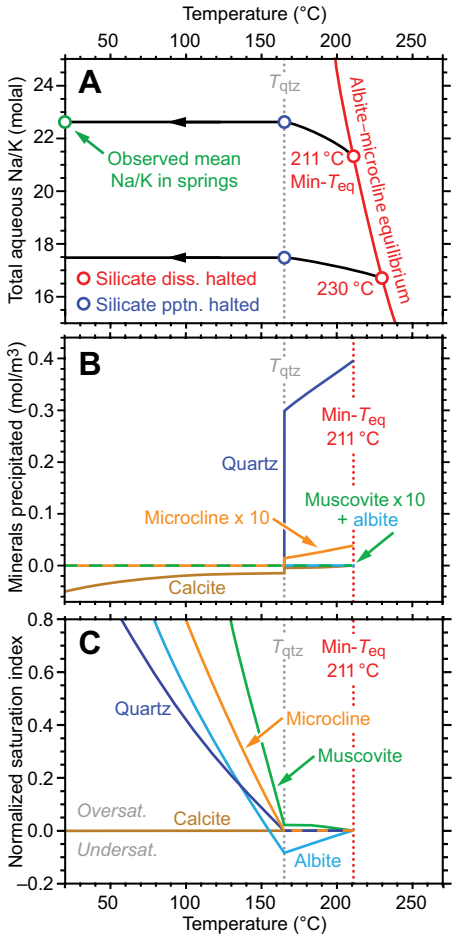

Figure 3. Numerical simulation of chemical evolution of thermal water upon upflow and cooling (explained in text). A: Observed Na/K ratio of thermal end-member water at its discharge site is reproduced if minimum temperature of equilibrium between water and wall rock (min-T_{eq}) is set at 211 °C. T_{qtz}—temperature at which cooling water departs from equilibrium with quartz; diss.—dissolution; pptn.—precipitation. B: Amounts of minerals precipitated in a nominal 40 yr period of upflow in mol per m^3 of porous rock. C: Saturation indices normalized to amount of Si in each mineral.

proven by the vastly weaker mineralization of the thermal springs (TDS ≤ 0.03 wt%). It follows that albite dissolution is the only source of Na in today's thermal waters. Finally, although we assumed in the simulations that the departure from complete water-rock equilibrium occurs at a unique temperature, the calculated min-T_{eq} remains a valid minimum even if, in reality, the kinetically controlled departure occurs over a temperature interval or if flow paths at several levels within the host fault contribute to the sampled spring waters.

IMPLICATIONS FOR DEEP METEORIC WATER INFILTRATION

Because the minimum deep temperature is 211 °C, the maximum temperature along the deep flow path of the Grimsel system is very

probably 230–250 °C or even higher. Given that the wall rocks along the flow path are the only heat source, their geothermal gradient of 25 °C/km implies that meteoric water must have penetrated to at least 9–10 km depth. To our knowledge, both this depth and deep-fluid temperature are the highest inferred from spring analyses at any active orogenic geothermal system worldwide. Hot springs elsewhere in similar structural and topographic settings with normal background geotherms (<30 °C/km) typically reveal min-T_{eq} < 150 °C and hence lower penetration depths, such as in the Canadian Rocky Mountains (Grasby and Hutcheon, 2001), the Qilian Mountains in China (Stober et al., 2016), the Pyrenees in Spain (Asta et al., 2010), and other locations in the Swiss Alps (Sonney and Vuataz, 2009). In comparison, more active orogens with high geothermal gradients yield higher min-T_{eq} values, such as the 200 °C temperature inferred from springs on the Alpine fault in New Zealand (Reyes et al., 2010). There, the extreme rock uplift rates (≤10 mm/yr) constitute an important mechanism of heat transport (generating geotherms ≥60 °C/km; Allis and Shi, 1995) in addition to topography-driven circulation of meteoric water (Sutherland et al., 2017). The higher temperature inferred for the base of the Grimsel Pass system is therefore all the more impressive, because with its low background geotherm and low exhumation rate (~1 mm/yr) typical of a waning orogen, little anomalous heat is being brought to the surface by the country rocks themselves.

Whereas the structural setting of the Grimsel geothermal system along a deep-reaching, strike-slip fault is not unusual, its properties are unusually favorable for application of Na-K solute geothermometry, and its modest background geotherm maximizes estimates of water penetration depth. The lower min-T_{eq} values found in similar settings in other orogens are therefore more likely to reflect local complications in methodology (e.g., Ferguson and Grasby, 2009; Peiffer et al., 2014) rather than shallower depths of meteoric water penetration. Similarly, sites with higher background geotherms will yield shallower minimum constraints on the depth of water penetration.

These conclusions imply that, first, the thermal anomalies associated with orogenic geothermal systems worldwide may have been systematically underestimated. Far more enthalpy may be accessible for geothermal energy exploitation within the thermal plumes around the upflow zones than previously thought. Second, our evidence that meteoric water penetrates down faults to 9–10 km depth calls for reassessment of the way in which such incursion influences seismicity. In the Grimsel area, for example, 33 of the 38 magnitude 0.1–2.5 earthquakes recorded since A.D. 1971 had focal depths shallower than 10 km (Belgrano et al., 2016, and references therein). Involvement of meteoric water in seismicity therefore seems very likely, although with the local brittle-ductile transition situated at 15–20 km depth (Viganò and Martin, 2007), there is no evidence for penetration of meteoric water into the ductile regime below Grimsel Pass.

ACKNOWLEDGMENTS

We acknowledge support from the Swiss Competence Center for Energy Research–Supply of Electricity (SCCER-SoE) and Swiss National Science Foundation NRP70 Grant 407040_153889 to Diamond. Grant Ferguson, Mark Reed, and an anonymous reviewer kindly provided constructive comments.

REFERENCES CITED

Allis, R.G., and Shi, Y., 1995, New insights to temperature and pressure beneath the central Southern Alps, New Zealand: New Zealand Journal of Geology and Geophysics, v. 38, p. 585–592, https://doi.org/10.1080/00288306.1995.9514687.

Asta, M.P., Gimeno, M.J., Auqué, L.F., Gómez, J., Acero, P., and Lapuente, P., 2010, Secondary processes determining the pH of alkaline waters in crystalline rock systems: Chemical Geology, v. 276, p. 41–52, https://doi.org/10.1016/j.chemgeo.2010.05.019.

Belgrano, T.M., Herwegh, M., and Berger, A., 2016, Inherited structural controls on fault geometry, architecture and hydrothermal activity: An example from Grimsel Pass, Switzerland: Swiss Journal of Geosciences, v. 109, p. 345–364, https://doi.org/10.1007/s00015-016-0212-9.

Egli, D., Glotzbach, C., Valla, P., Berger, A., and Herwegh, M., 2018, Low-temperature thermochronometry (apatite and zircon (U-Th)/He) across an active hydrothermal zone (Grimsel Pass, Swiss Alps): Geophysical Research Abstracts, v. 20, p. 12107.

Ferguson, G., and Grasby, S.E., 2009, What do aqueous geothermometers really tell us?: Geofluids, v. 9, p. 39–48, https://doi.org/10.1111/j.1468-8123.2008.00237.x.

Giggenbach, W.F., 1988, Geothermal solute equilibria: Derivation of Na-K-Mg-Ca geoindicators: Geochimica et Cosmochimica Acta, v. 52, p. 2749–2765, https://doi.org/10.1016/0016-7037(88)90143-3.

Grasby, S.E., and Hutcheon, I., 2001, Controls on the distribution of thermal springs in the southern Canadian Cordillera: Canadian Journal of Earth Sciences, v. 38, p. 427–440, https://doi.org/10.1139/e00-091.

Herwegh, M., Berger, A., Baumberger, R., Wehrens, P., and Kissling, E., 2017, Large-scale crustal-block-extrusion during late Alpine collision: Scientific Reports, v. 7, p. 413, https://doi.org/10.1038/s41598-017-00440-0.

Hofmann, B.A., Helfer, M., Diamond, L.W., Villa, I.M., Frei, R., and Eikenberg, J., 2004, Topography-driven hydrothermal breccia mineralization of Pliocene age at Grimsel Pass, Aar massif, central Swiss Alps: Schweizerische Mineralogische und Petrographische Mitteilungen, v. 84, p. 271–302, https://doi.org/10.5169/seals-63750.

Menzies, C.D., Teagle, D.A.H., Craw, D., Cox, S.C., Boyce, A.J., Barrie, C.D., and Roberts, S., 2014, Incursion of meteoric waters into the ductile regime in an active orogen: Earth and Planetary Science Letters, v. 399, p. 1–13, https://doi.org/10.1016/j.epsl.2014.04.046.

Peiffer, L., Wanner, C., Spycher, N., Sonnenthal, E.L., Kennedy, B.M., and Iovenitti, J., 2014, Multicomponent vs. classical geothermometry: Insights from modeling studies at the Dixie Valley geothermal area: Geothermics, v. 51, p. 154–169, https://doi.org/10.1016/j.geothermics.2013.12.002.

Pfeifer, H.R., Sanchez, A., and Degueldre, C., 1992, Thermal springs in granitic rocks from the Grimsel Pass (Swiss Alps): The late stage of a hydrothermal system related to Alpine orogeny, *in* Kharaka, Y.K., and Maest, A.S., eds., Proceedings of Water-Rock Interaction WRI–7, Park City, Utah: Rotterdam, Netherlands, A.A. Balkema, p. 1327–1330.

Raimondo, T., Clark, C., Hand, M., Cliff, J., and Anczkiewicz, R., 2013, A simple mechanism for mid-crustal shear zones to record surface-derived fluid signatures: Geology, v. 41, p. 711–714, https://doi.org/10.1130/G34043.1.

Reyes, A.G., Christenson, B.W., and Faure, K., 2010, Sources of solutes and heat in low-enthalpy mineral waters and their relation to tectonic setting, New Zealand: Journal of Volcanology and Geothermal Research, v. 192, p. 117–141, https://doi.org/10.1016/j.jvolgeores.2010.02.015.

Simmons, S., and Browne, P.R.L., 2000, Hydrothermal minerals and precious metals in the Broadlands-Ohaaki geothermal system: Implications for understanding low-sulfidation epithermal environments: Economic Geology and the Bulletin of the Society of Economic Geologists, v. 95, p. 971–999, https://doi.org/10.2113/gsecongeo.95.5.971.

Sonney, R., and Vuataz, F.-D., 2009, Numerical modelling of Alpine deep flow systems: A management and prediction tool for an exploited geothermal reservoir (Lavey-les-Bains, Switzerland): Hydrogeology Journal, v. 17, p. 601–616, https://doi.org/10.1007/s10040-008-0394-y.

Stober, I., Zhong, J., Zhang, L., and Bucher, K., 2016, Deep hydrothermal fluid-rock interaction: The thermal springs of Da Qaidam, China: Geofluids, v. 16, p. 711–728, https://doi.org/10.1111/gfl.12190.

Sutherland, R., Townend, J., Toy, V., et al., 2017, Extreme hydrothermal conditions at an active plate-bounding fault: Nature, v. 546, p. 137–140, https://doi.org/10.1038/nature22355.

Viganò, A., and Martin, S., 2007, Thermorheological model for the European central Alps: Brittle-ductile transition and lithospheric strength: Terra Nova, v. 19, p. 309–316, https://doi.org/10.1111/j.1365-3121.2007.00751.x.

Waber, H.N., Schneeberger, R., Mäder, U.K., and Wanner, C., 2017, Constraints on evolution and residence time of geothermal water in granitic rocks at Grimsel (Switzerland): Procedia Earth and Planetary Science, v. 17, p. 774–777, https://doi.org/10.1016/j.proeps.2017.01.026.

Wanner, C., Peiffer, L., Sonnenthal, E., Spycher, N., Iovenitti, J., and Kennedy, B.M., 2014, Reactive transport modeling of the Dixie Valley geothermal area: Insights on flow and geothermometry: Geothermics, v. 51, p. 130–141, https://doi.org/10.1016/j.geothermics.2013.12.003.

Xu, T., Sonnenthal, E.L., Spycher, N., and Zheng, L., 2014, TOUGHREACT V3.0-OMP Reference Manual: A Parallel Simulation Program for Non-Isothermal Multiphase Geochemical Reactive Transport. LBNL Manual: http://esd1.lbl.gov/FILES/research/projects/tough/documentation/TOUGHREACT_V3-OMP_RefManual.pdf (accessed July 2018).

Printed in USA